Loss of Neil3, the major DNA glycosylase activity for removal of hydantoins in single stranded DNA, reduces cellular proliferation and sensitizes cells to genotoxic stress

Veslemøy Rolseth, Silje Zandstra Krokeide, David Kunke [1], Christine Gran Neurauter, Rajikala Suganthan, Yngve Sejersted, Gunn Annette Hildrestrand, Magnar Bjørås, Luisa Luna *

Department of Microbiology and CMBN, University of Oslo, Oslo University Hospital, Rikshospitalet, PO Box 4950 Nydalen, N-0424 Oslo, Norway

ABSTRACT

7,8-Dihydro-8-oxoguanine (8-oxoG) is one of the most common oxidative base lesions in normal tissues induced by a variety of endogenous and exogenous agents. Hydantoins are products of 8-oxoG oxidation and as 8-oxoG, they have been shown to be mutagenic lesions. Oxidative DNA damage has been implicated in the etiology of various age-associated pathologies, such as cancer, cardiovascular diseases, arthritis, and several neurodegenerative diseases. The mammalian endonuclease VIII-like 3 (Neil3) is one of the four DNA glycosylases found to recognize and remove hydantoins in the first step of base excision repair (BER) pathway. We have generated mice lacking Neil3 and by using total cell extracts we demonstrate that Neil3 is the main DNA glycosylase that incises hydantoins in single stranded DNA in tissues. Using the neurosphere culture system as a model to study neural stem/progenitor (NSPC) cells we found that lack of Neil3 impaired self renewal but did not affect differentiation capacity. Proliferation was also reduced in mouse embryonic fibroblasts (MEFs) derived from $Neil3^{-/-}$ embryos and these cells were sensitive to both the oxidative toxicant paraquat and interstrand cross-link (ICL)-inducing agent cisplatin. Our data support the involvement of Neil3 in removal of replication blocks in proliferating cells.

© 2013 Elsevier B.V. Open access under CC BY-NC-ND license.

1. Introduction

Oxidative DNA damage is generated by a variety of reactive oxygen species (ROS), which are produced through normal cellular metabolism and by various environmental mutagens and dietary factors [1]. Oxidative DNA lesions are of significant interest, due to their implications in mutagenesis, carcinogenesis, aging, and neurodegeneration [2–6]. These lesions are repaired *via* the base excision repair (BER) pathway which recognizes and removes damaged bases from DNA [7,8]. Mammalian cells possess at least five DNA glycosylases with overlapping substrate specificity that recognize and remove oxidative DNA lesions: OGG1/Ogg1, NTHL1/Nthl1 and three *E. coli* Fpg and Nei orthologs in mammalian cells, named NEIL1,2,3/Neil1, 2 and 3 [7,8]. The prevalent oxidative DNA lesion, 7,8-dihydro-8-oxoguanine (8-oxoG) is subject to further oxidation to form the hydantoin products spiroiminodihydantoin (Sp) and guanidinohydantoin (Gh) [9–13]. The hydantoin lesions have been shown *in vitro* and *in vivo* to be highly mutagenic [14]. Sp and Gh

are removed by NTHL1/Nthl1 and the NEILs/Neils but not by OGG1/Ogg1 [15–20].

DNA glycosylases are widely expressed in all organs and in most cells; conversely NEIL3/Neil3 has a characteristic expression pattern limited to a few organs and specific cells [21–31]. Human NEIL3 is highly expressed in thymus and testis, in tumor tissues and in highly proliferative cells [24,30,32]. Mouse Neil3 is highly expressed in hematopoietic tissue, during embryonic development and in stem/progenitor rich regions in the brain such as the subventricular zone and the dentate gyrus of hippocampus [27,29,30]. Targeted deleted mice have been generated for Ogg1, Nthl1, Neil1 and Neil3 and share the fact that they are viable, fertile and with only subtle phenotypes as single or even double knock outs [27,33–39]. However, exposure of these mice toward insults such as brain ischemia has started to reveal various detrimental effects [39–41].

In this paper we demonstrate that Neil3 is the key enzyme in cell extracts for removal of hydantoins in single stranded context. Further, there are no major differences in the brain anatomy of newborn $Neil3^{+/+}$ and $Neil3^{-/-}$ animals. However, using the neurosphere assay to study neural/progenitor stem cell (NSPC) behavior *in vitro*, we showed that self renewal but not differentiation capacity was affected in $Neil3^{-/-}$ derived neurospheres. Finally, Neil3 loss sensitizes mouse

---

* Corresponding author. Tel.: +47 23 07 40 69; fax: +47 23 07 40 61.
E-mail address: luisa.luna@rr-research.no (L. Luna).
[1] Present address: Institute for Surgical Research, University of Oslo, Oslo University Hospital, Rikshospitalet, PO Box 4950 Nydalen, N-0424 Oslo, Norway.

embryonic fibroblast (MEF) cells to the oxidative toxicant paraquat and the interstrand cross-link (ICL)-inducing agent cisplatin.

2. Materials and methods

2.1. Animals

Neil3 KO mice were generated as previously described [39]. Experimental procedures were approved by the Norwegian Animal Research Authority.

2.2. DNA glycosylase assay

Whole-cell protein extracts from $Neil3^{+/+}$ and $Neil3^{-/-}$ were made from brain, heart, thymus and spleen of newborn mice. The organs were first scalpel macerated and then homogenized in lysis buffer (50 mM MOPS, 200 mM KCl, 0,1% Triton X-100, 1 mM EDTA, 1 mM DTT, and 2 mM PMSF) using a motorized pestle. After 30 min incubation on ice, the extracts were frozen on ethanol–dry ice/thawed at 30 °C three times. Cell debris was removed by 15 min centrifugation at 13,000 rpm. The protein concentration was measured using Bradford assay.

Oligonucleotides containing the base lesions: 5-ohC ($5'$gcatgcctgcacgg [5-ohC]catggccagatccccgggtaccgag$3'$) (Operon), Sp or Gh ($5'$tgttcatcatgcg tc[Gh/Sp]tcggtatatcccat$3'$) (a kind gift from Prof. Cynthia J. Burrows, Department of Chemistry, University of Utah) were ^{32}P-endlabeled by T4 PNK (New England Biolabs) and [γ-^{32}P]adenosine triphosphate (Perkin Elmer) by incubation for 30 min at 37 °C. PNK was inactivated by heating at 80 °C. Complementary oligonucleotides, containing a C opposite Gh and Sp or a G opposite 5-ohC were annealed by heating the sample to 90 °C for 2 min followed by slow cooling to room temperature to generate double stranded substrates. The oligonucleotides were purified by 20% native polyacrylamide gel electrophoresis, visualized by phosphorimaging (Typhoon 9410 (Molecular Dynamics)), isolated from the gel, eluted in dH$_2$O and stored at 4 °C. Incision activities were assayed in a 10 μl reaction mixture containing 10 fmol radiolabeled substrate, 50 mM MOPS pH 7.5, 1 mM EDTA, 5% glycerol, 1 mM DTT and 4 μg whole-cell protein extracts at 37 °C for 60 min. The enzymatic reaction was terminated by adding 10 μl formamide solution (80% formamide, 10 mM EDTA, bromophenol blue and xylene cyanol) and analyzed on 20% polyacrylamide/7 M urea gel followed by phosphorimaging. Incision activity was calculated using the ImageQuant v5.0 software (Molecular Dynamics).

2.3. Total RNA isolation, cDNA synthesis and real-time qRT-PCR

Total RNA was isolated from $Neil3^{+/+}$ and $Neil3^{-/-}$ brain, heart, thymus and spleen of newborn mice using the RNeasy minikit (Qiagen) following the manufacturer's instructions. The RNA was further purified by phenol/chloroform extraction and RNA was treated with TurboDNase (Applied Biosystems). The purity of RNA was controlled by absorbance (260/280 nm and 260/230 nm) measurements using Nanodrop Spectrophotometer. cDNA was synthesized from 50 ng RNA in 20 μl reaction samples using the High-Capacity cDNA Reverse Transcription kit (Applied Biosystems). Real-time qRT-PCR was performed in 20-μl reactions containing 10 ng of cDNA and 100 nM primers using the Power SYBR Green PCR master mix and the Step One Plus real-time PCR system (Applied Biosystems) according to the system and kit instructions. The expression of Gapdh was used as endogenous control and standard curves for primers were assayed on each plate. Relative gene expression was calculated using the relative standard curve method. The experiment was performed three times with RNA isolated from three different mice. All samples were run in triplicates. Primers are listed in Table 1.

Table 1
Primers used in real-time qRT-PCR.

Target	Sequence 5′→3′	Acc. nr.
Nhtl1	Right primer: TGGTCCACCTCAGTCTGTTG	NM_008743
	Left primer: CACACTTGGCTATGGCTGTG	
Neil1	Right primer : GAGATCCTGTACCGGCTGAAGA	NM_028347
	Left primer : GGTTCTGTAGTTTGGCCTTGATCT	
Neil2	Right primer: TTCCCTGTATAGGCTGTGGG	NM_201610
	Left primer : GTCTCTGTGGCCTCCAGGATG	
Neil3	Right primer: GGGCAACATCATCAAAAATGAA	NM_146208
	Left primer : CTGTTTGTCTGATAGTTGACACACCTT	
Gapdh	Right primer: CCAAGGTCATCCATGACAACTT	
	Left primer : AGGGGCCATCCACAGTCTT	

2.4. Immunohistochemistry

$Neil3^{+/+}$ and $Neil3^{-/-}$ P0 mice were transcardially perfused with PBS and then 4% PFA. For BrdU analysis, newborn mice were injected intraperitonal with 100 μg/gram bodyweight BrdU (Sigma) in PBS (room temperature) 2 h before perfusion. Brains were removed and post fixed in PFA for at least 24 h at 4 °C before being dehydrated and embedded in paraffin. Sagittal sections of 4 uM were cut on a microtome and sections from the same brain area of $Neil3^{+/+}$ and $Neil3^{-/-}$ were placed on the same glass slides to secure equal immunohistochemistry procedure for both genotypes. Antigen retrieval was performed using citrate buffer, pH 6.0, and heating for 20 min in a microwave oven. Sections were blocked with 5% BSA and 5% goat serum in PBS with 0.1% Tween for 1 h before treatment with primary antibody for 24 h at 4 °C in 0.5% goat serum, 0.5% BSA, and in PBS with 0.1% Tween. After washing in 0.1% Tween in PBS the sections were treated with secondary antibody for 1 h at room temperature. For BrdU staining, DNA was denatured with 1 M HCl for 10 min on ice and then in 2 M HCl 10 min in room temperature and further incubation for 20 min at 37 °C. Then the sections were neutralized in PBS before blocking. Nuclei were counterstained with DAPI (Sigma). Sections were visualized using an Axioplan2 Zeiss fluorescence microscope and BrDU cells were quantified with ImageJ (National Institutes of Health).

$Neil3^{+/+}$ and $Neil3^{-/-}$ neurospheres derived from newborn whole brain were pelleted, suspended in plasma and thrombine at day 7 after 2nd passage, fixated, dehydrated, paraffin embedded, sectioned and stained. Staining was performed as described above.

The primary antibodies used were: mouse anti-Nestin 1:200 (MAB353, Millipore); mouse anti-GFAP 1:400 (G9838; Invitrogen); rabbit anti-doublecortin 1:2000 (ab18723; AbCam); mouse anti-doublecortin 1:500 (611706; BD Transduction); mouse anti-β-tubulin subtype III (Tuj1) 1:100 (MAB1195; R&D Systems) and rat anti-BrdU 1:1000 (ab6326; AbCam). Secondary antibodies used were Alexa Fluor 594 anti-mouse, Alexa Fluor 488 anti-rabbit and Alexa Fluor 594 anti-rat at 1:500 dilutions (Molecular Probes/Invitrogen).

2.5. Neurosphere propagation, colony forming assay and differentiation

Neurospheres were prepared from $Neil3^{+/+}$ and $Neil3^{-/-}$ forebrains of newborn mice, cultured and propagated as previously described, with some modifications [42,43]. Cells were cultured in serum free Neurobasal-A medium (Gibco/Invitrogen) supplemented with 2% B-27 (Gibco), 2 mM glutamine (GlutaMAX; Gibco) and penicillin/ streptomycin (Pen-Strep 100X; MP Biomedicals Fisher Scientific), 20 ng/ml hEGF (R&D Systems) and 10 ng/ml hFGF-2 (MACS; Milteney Biotech) at a concentration of 20,000 live cells/ml. Neurosphere cultures were grown for 7 days and then trypsinized and filtered through a 70 uM mesh before being resuspended in medium for propagation, exposure experiments, colony forming assays and differentiation.

For colony forming assays, single cells were seeded into 96 well plates at 500 cells per well and grown for 11 days before colonies

were counted by GelCount™ (Oxford Optronix). Only spheres > 50 μm were counted.

For differentiation, single cells from spheres were plated in 24 well poly-L-lysine coated plates at a concentration of 150,000 cells/ml in medium without EGF and incubated for 5 days. Cells were fixed in 4% PFA for 10 min, permeabilized with 0.1% Triton X-100 in PBS for 10 min and stained with Nestin, GFAP, Tuj1 and DCX as described for immunohistochemistry. Cells were analyzed in a Zeiss Axiovert 200M Microscope using AxioVision 4.6 software.

2.6. Primary mouse embryonic fibroblasts and exposure experiments

Primary mouse embryonic fibroblasts (MEFs) were generated from 15,5 days old $Neil3^{+/+}$ and $Neil3^{-/-}$ embryos. Limbs were removed from embryos and the tissue was chopped into small pieces and cell suspension was made using a pipette. MEFs were grown in DMEM medium (Gibco/Invitrogen) supplemented with 10% serum, 2 mM glutamine (GlutaMAX, Gibco) and penicillin/streptomycin as before (complete medium). Cells grown for 7–8 days were trypsinized and frozen down in complete medium with 10% DMSO as stock. Frozen aliquots were taken up and grown in complete medium for 2–4 days before using them for proliferation capacity and survival assays.

Primary MEF cells were seeded in 96 well plates at a concentration of 10 000 cells/well, incubated for 4 h and treated with 0, 25, 50 and 75 μM paraquat or 0, 5, 10 and 20 μM of cisplatin for 24 h. 5 mg/ml MTT was added to cells for 4 h and then 100 μl solubility solution was added to each well and incubated at 37 °C over night before measurement of OD at 590 and 670. Results are presented as 590–670 OD minus OD for only medium, % of control.

3. Results

3.1. Impaired removal of hydantoins in tissues of newborn Neil3$^{-/-}$ mice

The expression of $Neil1$, $Neil2$, $Neil3$ and $Nthl1$ has been examined by different methods in various tissues, during embryonic development and at different ages [27,29,30,44]. In this report we have investigated by real-time qRT-PCR the levels of $Neil1$, $Neil2$, $Neil3$ and $Nthl1$ in thymus, spleen, heart and brain from $Neil3^{+/+}$ and $Neil3^{-/-}$ newborn mice (Fig. 1A). As seen in Fig. 1A, $Neil3$ was highly expressed in thymus and spleen, but barely detected in $Neil3^{+/+}$ brain and heart. In contrast, the expression levels of $Neil1$ and $Neil2$ were relatively high in thymus compared to the rest of the organs investigated. For $Nthl1$, the expression was more homogeneous with spleen having the highest levels (Fig. 1A).

To investigate the effects of $Neil3$ disruption, nicking activities for single and double stranded Gh and Sp and double stranded 5-ohC were measured in total cell extracts from newborn $Neil3^{+/+}$ and $Neil3^{-/-}$ thymus, spleen, heart and brain. As seen in Fig. 1B, nicking activity on double stranded substrates was readily detected in all tissues and there was no difference between $Neil3^{+/+}$ and $Neil3^{-/-}$. Nicking activity on single stranded substrates was persistently lower compared to the nicking activity on double stranded substrates in all tissues. Notably, the incision activity on single stranded Sp and Gh was reduced in all the $Neil3^{-/-}$ extracts as compared to $Neil3^{+/+}$ extracts. To investigate whether the activity on single stranded hydantoins was derived primarily from the Neil3 protein we performed a sodium cyanoborohydride (NaCNBH$_3$) trapping assay. This reagent reduces the Schiff base intermediate and provokes the formation of a stable cross-link between enzyme and DNA. The DNA–protein complex can be visualized as a band on SDS/PAGE gels [45,46]. Migration of the DNA–protein complexes depends on the size of the protein and the nature of the DNA substrate. We tested fractions of purified full-length NEIL3 (MW: 68 kDa), core-NEIL3 (MW: 34 kDa) [47] and purified $E.$ $coli$ Fpg (MW: 30.2 kDa, Nei (MW: 29.7 kDa) and Nth (MW: 23 kDa) in the borohydride-dependent trapping assay to AP site-containing ssDNA. The slowest migrating band

corresponded to the 68 kDa partially purified full-length NEIL3, while the faster migrating bands corresponded to the 23–34 kDa core-NEIL3, and $E.$ $coli$ Fpg, Nei and Nth proteins (Supplementary Fig. S1). For the double-stranded substrates, there were several bands indicating the presence of different trapped proteins, however the slowest migrating band was absent in the $Neil3^{-/-}$ extracts (Fig. 1C). For the single-stranded substrates fewer bands were detected and again, the slowest migrating band was absent in the $Neil3^{-/-}$ extracts (Fig. 1C). A size difference on the trapped bands between ss and ds substrates was observed. Such migrating differences have been observed for purified NEIL1 and NEIL2 in similar trapping experiments using Sp and Gh substrates in ss and ds contexts [16]. These results indicated that the slowest migrating band observed in the $Neil3^{+/+}$ extracts corresponded to the Neil3–DNA complex. Both the expression analysis and activity assays presented support the conclusion that Neil3 was the main enzyme responsible for the removal of hydantoins in single stranded substrates.

3.2. Neil3 loss does not affect brain size or architecture

In light of the restricted pattern of $Neil3$ expression during mouse brain embryonic development we set out to examine the morphology and cellular composition of P0 brains isolated from $Neil3^{+/+}$ and $Neil3^{-/-}$ mice. At this stage, neurogenesis, which begins early in embryonic life, is largely complete, however, in certain locations neurogenesis persists into adulthood and any major defect in the structural organization can be readily detected [48–50].

To investigate the cellular composition and differentiation pattern, we analyzed serial sagittal sections with various antibodies specific for various stages of differentiation: nestin, an intermediate filament protein found in noncommitent NSCs and GFPA an intermediate filament in astrocytes. There was no difference in the expression of the tested antibodies between $Neil3^{-/-}$ and $Neil3^{+/+}$ P0 brains (Fig. 2A).

To investigate the proliferation state, we used four different markers with specificity in different cell cycle phases: BrdU, 5-bromo-2-deoxyuridine, a thymidine analogue that is incorporated into DNA during the S-phase of the cell cycle [51]; Ki67, a nuclear antigen which is expressed in all cell cycle phases except for G_0 [52,53]; PCNA, the proliferating cell nuclear antigen, a non-histone protein associated with the DNA polymerase [54]; and pHH3, the phosphorylated histone H3, a marker for G_2/M of the cell cycle [55]. No differences could be seen with any of these markers in the dentate gyrus of the hippocampus (Fig. 2B, example of BrdU) or in the walls of the lateral ventricles (data not shown) between the two genotypes. In summary, we did not detect any effect of Neil3 deficiency on gross brain morphology, cell composition or state of proliferation in the P0 animals.

3.3. Neurospheres from forebrain of Neil3$^{-/-}$ newborn mice exhibit reduced proliferation but have normal differentiation capacity

We next established neurosphere cultures from forebrain of $Neil3^{+/+}$ and $Neil3^{-/-}$ newborn mice and examined neurosphere composition, self-renewal and differentiation capacity. $Neil3^{+/+}$ and $Neil3^{-/-}$ neurospheres exhibited typical morphology of densely packed cells with a regular rim and well defined spherical shape and were of equal size. To investigate whether there was a difference between the composition of $Neil3^{+/+}$ and $Neil3^{-/-}$ neurospheres, immunohistochemical phenotypization was carried out. As seen in Fig. 3, no differences were detected with the antibodies used; Nestin, Tuj1, GFAP and DCX, doublecortin, a microtubule-associated protein transiently expressed in proliferating and migrating neuronal progenitors during development [56,57].

To assess self-renewal capability, $Neil3^{+/+}$ and $Neil3^{-/-}$ neurospheres were serially dissociated into single cells to generate secondary, tertiary and up to septenary neurospheres. The $Neil3^{-/-}$ derived neurospheres formed fewer spheres suggesting that the self-renewing activity was impaired (Fig. 4A). To examine multipotentiality, we analyzed the effect of
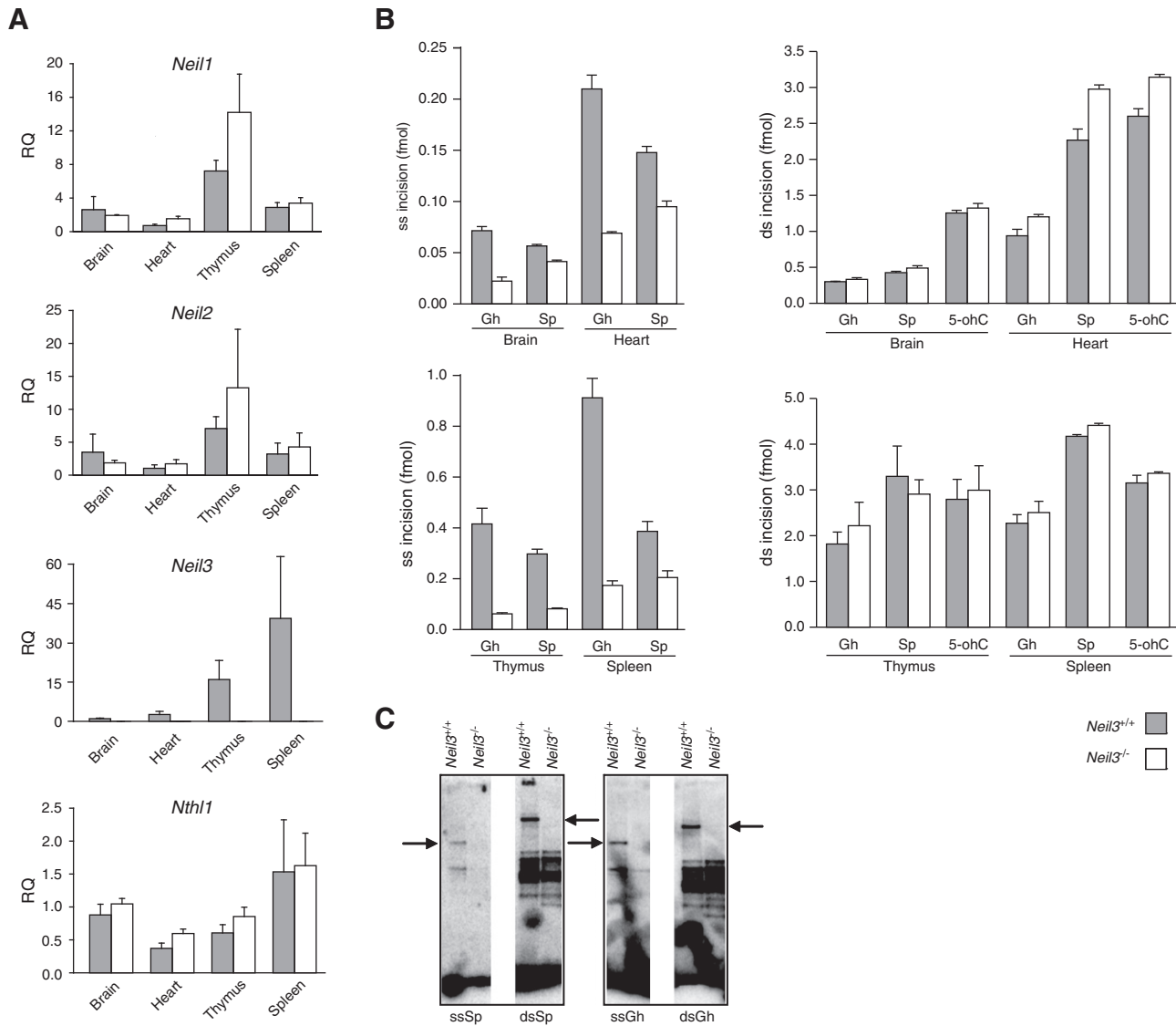
Fig. 1. Relative expression and DNA glycosylase incision activities in organs of P0 *Neil3*$^{+/+}$ and *Neil3*$^{-/-}$ mice. (A) Relative expression of *Neil1*, *Neil2*, *Neil3* and *Nthl1*. Total RNA was extracted from brain, heart, thymus and spleen, real-time qRT-PCR was performed and the relative expression was normalized to the expression of Gapdh in the same samples. Values represent mean $+/-$ SEM of three individual experiments/mice. All experiments were performed in triplicates. (B) Quantification of DNA glycosylase activities of *Neil3*$^{+/+}$ and *Neil3*$^{-/-}$ P0 mice organ extracts. Incision activity of brain, heart, thymus and spleen extracts on single-stranded (Sp and Gh) and double stranded (Sp, Gh and 5-ohC) substrates. 4 μg of extracts was incubated with 10 fmol ^{32}P-labelled oligonucleotide with a base lesion for 1 h at 37 °C. Products were resolved by PAGE. Results were visualized by phosphorimaging. Incision activities were calculated from the amount of radioactivity in the products relative to the total in the lane. Values represent mean $+/-$ SEM of three independent experiments/mice each performed in triplicates. (C) Probing for covalent protein–DNA intermediates by NaCNBH$_3$ reduction. 4 μg of *Neil3*$^{+/+}$ and *Neil3*$^{-/-}$ thymus extracts was incubated with 10 fmol ^{32}P-labelled oligonucleotide with a base lesion in the presence of NaCNBH$_3$ for 1 h at 37 °C. Protein–DNA complexes were separated by 10% Tricine-SDS-PAGE and analyzed by phosphorimaging.

Neil3 loss on differentiation using an *in vitro* differentiation assay, whereby single-cell suspensions from secondary or higher passages were induced to differentiate when plated at a high density in adherent conditions in the absence of EGF for 5 days. The cells were immunostained to assess the differentiation into immature neurons (Tuj1) and astrocytes (GFAP) (Fig. 4B). We noted no differences between the two genotypes.

3.4. Proliferation of Neil3$^{-/-}$ primary embryonic fibroblasts is abridged and show sensitivity toward DNA damaging agents

Proliferation capacity and cell survival was examined in primary MEFs derived from E15.5 *Neil3*$^{+/+}$ and *Neil3*$^{-/-}$ embryos. We first examined the proliferative capacity of *Neil3*$^{+/+}$ and *Neil3*$^{-/-}$ primary MEFs and detected a diminished proliferative capacity of the *Neil3*$^{-/-}$ primary MEFs (Fig. 5A). As NEIL3 has been shown to partially complement an *E. coli* nth nei double mutant strain sensitive to hydrogen

peroxide [31] we therefore wanted to test whether the absence of Neil3 would sensitize cells to different genotoxic stress. As shown in Fig. 5B, primary *Neil3*$^{-/-}$ MEFs were more sensitive to paraquat than primary *Neil3*$^{+/+}$ MEFs supporting the notion that Neil3 is involved in repair of oxidative DNA lesions. Surprisingly, primary *Neil3*$^{-/-}$ MEFs were more sensitive to cisplatin than primary *Neil3*$^{+/+}$ MEFs, indicating a role in DNA crosslink repair.

4. Discussion

In this report we present evidence that *in vivo*, Neil3 is the main DNA glycosylase for the removal of hydantoins in single stranded substrates in four different tissues derived from newborn mice. *Neil3*$^{+/+}$ and *Neil3*$^{-/-}$ total cell extracts displayed no difference in the incision of double stranded substrates containing hydantoins, however incision in the single stranded context was reduced in the *Neil3*$^{-/-}$ extracts.
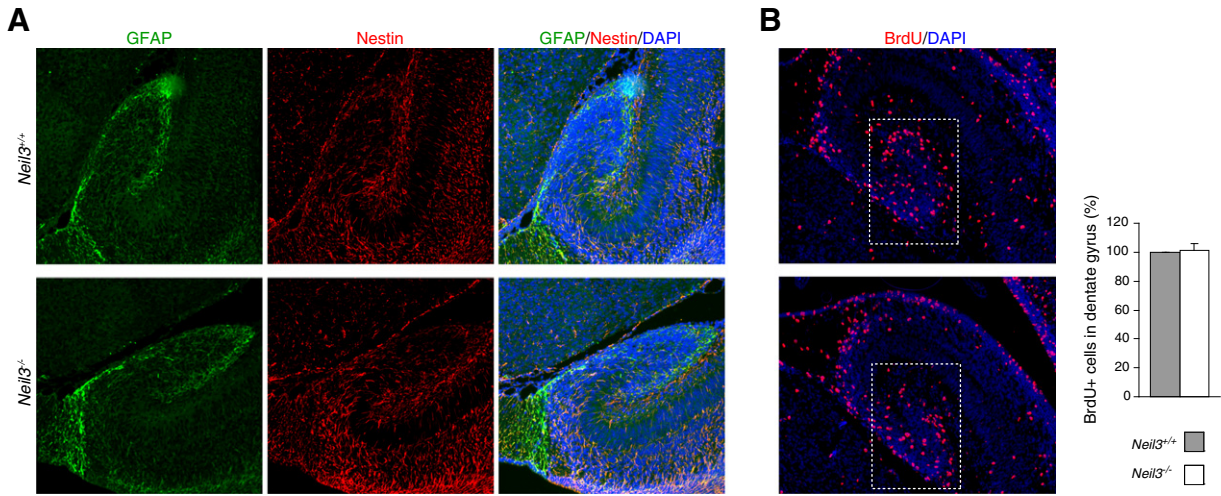
Fig. 2. Characterization of Neil3$^{+/+}$ and Neil3$^{-/-}$ P0 brains. (A) Photomicrographs showing representative double staining of GFAP (green) and Nestin (red) in Neil3$^{-/-}$ and Neil3$^{+/+}$ hippocampus from newborn mice. Nuclei were stained with DAPI (blue). (B) Photomicrographs showing representative BrdU labeled cells (red) in the dentate gyrus of Neil3$^{-/-}$ and Neil3$^{+/+}$ hippocampus. Nuclei were stained with DAPI (blue). (C) Quantification of BrdU positive cells in the dentate gyrus of Neil3$^{-/-}$ and Neil3$^{+/+}$ hippocampus.

Much work has been done to assess the removal of hydantoin lesions in different substrate contexts by the NEIL recombinant proteins. To sum up the results of various reports: NEIL1 is more efficient in removing hydantoins relative to other oxidized bases particularly in double stranded substrates, while NEIL2 is more efficient in single stranded substrates [15–17,19]. For Neil3 the data is more limited as much of the work has been done with a truncated Neil3 protein containing the DNA glycosylase domain (GD) but lacking the C-terminal domain and
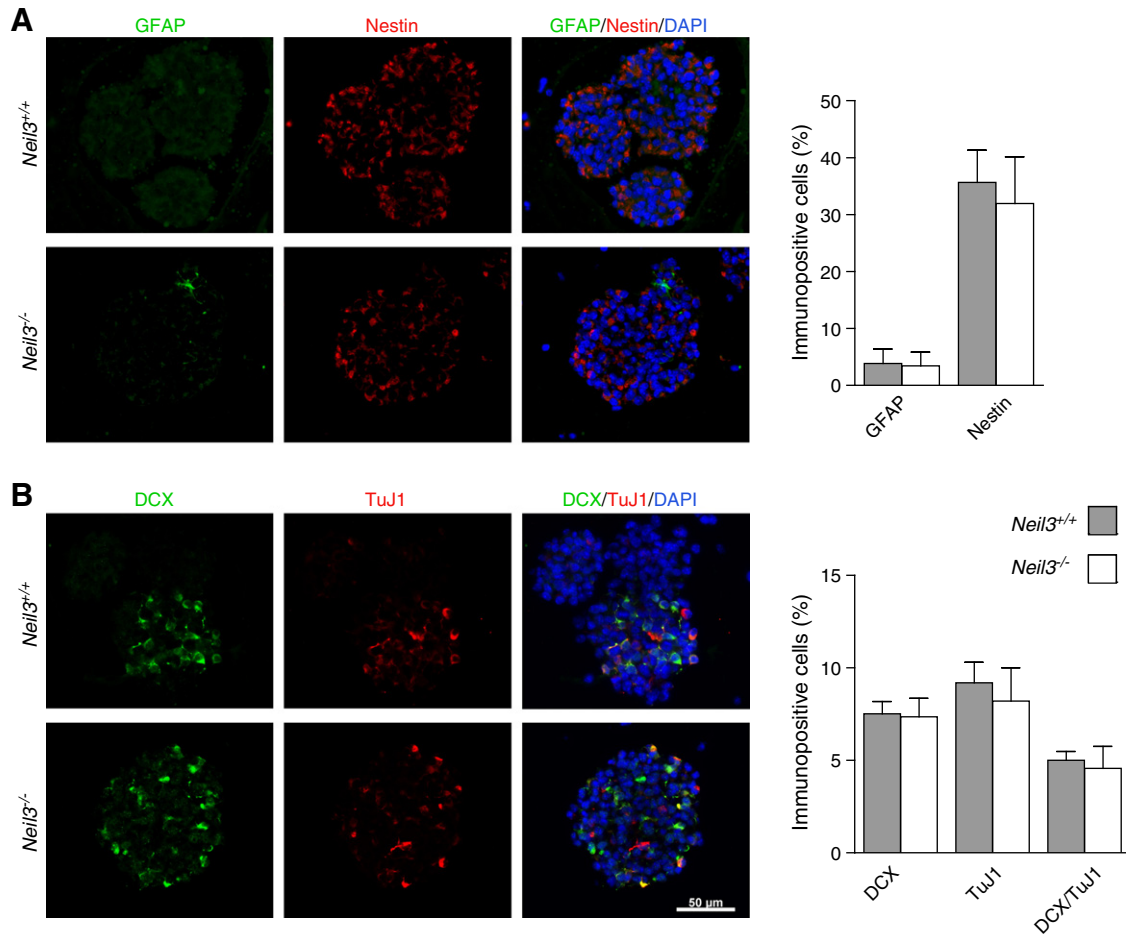

Fig. 3. Characterization of neurospheres derived from Neil3$^{+/+}$ and Neil3$^{-/-}$ P0 forebrains. (A) and (B) Photomicrographs illustrate the typical cellular composition in neurosphere sections. (A) Astrocytes (GFAP+) and neuronal progenitors (Nestin+). Very few astrocytes were present. (B) Neuronal progenitors (DCX+) and immature neurons (TuJ1+). Nuclei are stained with DAPI (blue). Quantification revealed no significant differences in cellular composition of sphere sections when comparing Neil3$^{-/-}$ cultures (n=6) and Neil3$^{+/+}$ cultures (n=6). Counting was performed in 6–8 spheres per culture and a total of 3399 Neil3$^{-/-}$ and 3507 Neil3$^{+/+}$ cells were analysed for each antibody. To avoid counting only in the periphery of a sphere, only sections>50 μm in diameter were included.
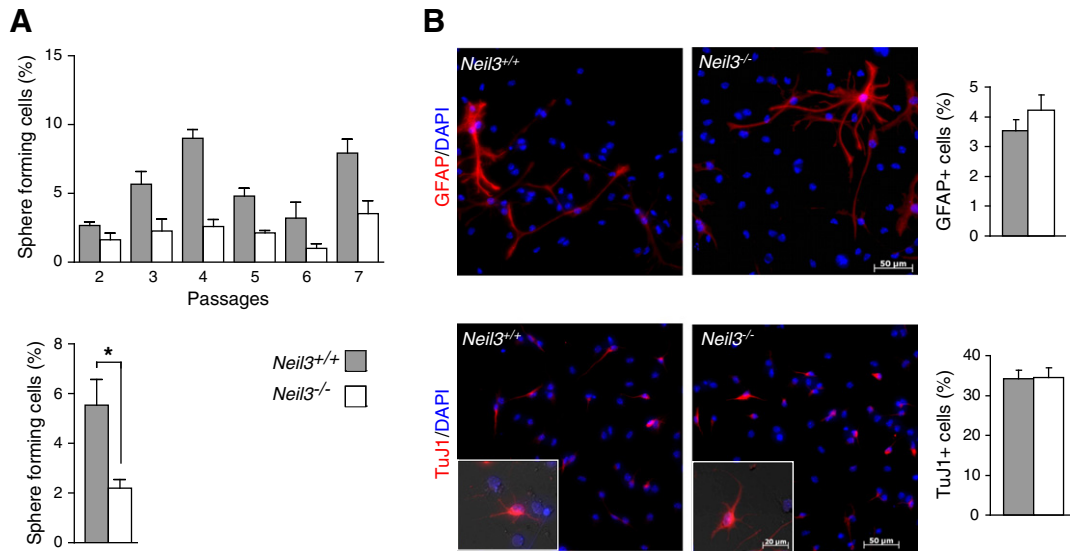
Fig. 4. Reduced self-renewal capacity but not differentiation potential of neurospheres derived from newborn forebrain of *Neil3*$^{+/+}$ and *Neil3*$^{-/-}$ animals. (A) Percentage of spheres formed from 500 plated cells at passage 2 to passage 7, day 11. Mean +/− SEM of 3 wells. * indicates p = 0.012 by Student's t-test. Average of spheres formed from passage 2–6. Mean +/− SEM of 6 experiments. * indicates p = 0.012 by Student's t-test. (B) Photomicrographs illustrate typical cells generated from neurospheres and differentiated into glia (stained with GFAP) and neurons (stained with Tuj1) from single cells. Nuclei were stained with DAPI (blue). Quantification revealed no significant differences in differentiation capacity when comparing *Neil3*$^{-/-}$ to *Neil3*$^{+/+}$.

a partially purified full length Neil3 protein [18,58]. These results showed that the enzymes were almost as active in hydantoin containing single- and double-stranded substrates. For endogenous NEIL3, we recently reported DNA incision activity on single stranded Gh substrate, however to our knowledge, this is the only report on the activity of any of the endogenous NEILs/Neils [32]. The incision activity results presented in this paper using *Neil3*$^{+/+}$ and *Neil3*$^{-/-}$ total cell extracts clearly showed that Neil3 is the main DNA glycosylase that incises Sp or Gh single stranded substrates.

The lack of Neil3 did not affect the overall macroscopic organization or size of the brain nor did Neil3 deficiency appear to have a major effect on proliferation or composition in the DG of the hippocampus or in the SVZ. Nevertheless, *Neil3*$^{-/-}$ derived neurospheres enriched for NSPCs exhibited reduced proliferation but normal capacity to differentiate under unstressed conditions. Decreased proliferative capacity has also been observed for neurospheres derived from the SVZ of 18 month *Neil3*$^{-/-}$ animals and in rat E15.5 (corresponding to mouse E13.6) derived neurospheres in which Neil3 was knocked down [59,60].
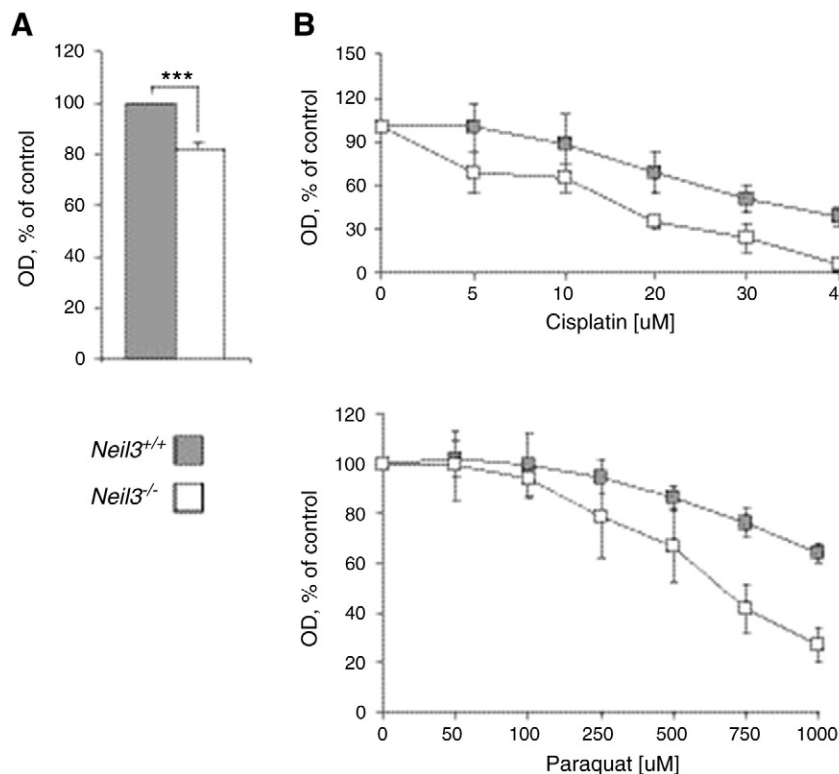

Fig. 5. *Neil3*$^{-/-}$ primary MEFs exhibited reduced proliferation and were sensitive toward paraquat and cisplatin treatment. (A) MTT assay of *Neil3*$^{-/-}$ and *Neil3*$^{+/+}$ primary MEFs with 5000 cells seeded in wells of 96 well plates (6 triplicates for each genotype). Results are mean OD (% of control) of three independent experiments. *** p < 0.0005. (B) MTT assay of *Neil3*$^{-/-}$ and *Neil3*$^{+/+}$ primary MEFs treated with increasing amounts of paraquat and cisplatin.

In contrast to our differentiation results, the expression of neuronal and astrocytic genes decreased in siNeil3 neurospheres compared to controls [60]. This discrepancy can be due to several differences between the experimental set up. The neurospheres were made by different methods and at different time points. Interestingly, siNeil3 neurospheres were made at a time corresponding in mice were there are high numbers of Neil3 positive cells as compared to newborn. This might influence the differentiation capacity. Second, the differentiation of the rat neurospheres has been enhanced with the addition of valproic acid which we did not use. There is now experimental evidence linking valproic acid to the generation of oxidative stress [61]. Thus, differentiation deficiency observed in siNeil3 neurospheres can be due to the treatment with valproic acid producing oxidative stress. Similarly, differentiation deficiency was observed for $Neil3^{-/-}$ neurospheres derived from brain subjected to ischemic insult [39]. Finally, differentiation has been assessed in different ways. We looked at the number of cells expressing different markers while the other report uses quantitative RT-PCR to assess differentiation.

$Neil3^{-/-}$ MEFs were sensitive toward paraquat and cisplatin. Both paraquat and cisplatin have been shown to induce oxidative stress; however the DNA damage spectra are quite different [62–64]. Cisplatin interacts with nucleophilic N7-sites of purine bases in DNA to form DNA interstrand (ICL) crosslinks [65,66]. The repair of ICLs requires the interplay of multiple pathways including nucleotide excision repair, homologous recombination, mismatch repair, Fanconi anemia signaling pathway and translesion synthesis [67,68]. NEIL1 has been shown to excise bulky psoralen-induced ICLs implicating BER in the repair of ICLs [69–71]. The authors proposed a model for replication-associated repair of psoralen-induced ICLs in which NEIL1 has a role excising the unhooked fragment in a three-stranded DNA structure [70]. Similarly, as (i) NEIL3 is highly expressed in S phase [32]; (ii) Neil3 excises base lesions in single stranded context; (iii) $Neil3^{-/-}$ MEFs are sensitive toward cisplatin treatment and (iv), the expression of Neil3 has been shown to be upregulated in breast cancer cells after cisplatin treatment [72], we would like to extend the suggested model to include Neil3 in replication-associated repair of cisplatin-induced ICLs. Additional experiments have to be done to elucidate the types of damage and the proteins involved in such a model.

Supplementary data to this article can be found online at http://dx.doi.org/10.1016/j.bbamcr.2012.12.024.

Acknowledgements

References

[1] M. Dizdaroglu, P. Jaruga, Mechanisms of free radical-induced damage to DNA, Free Radic. Res. 46 (2012) 382–419.
[2] J.E. Klaunig, L.M. Kamendulis, The role of oxidative stress in carcinogenesis, Annu. Rev. Pharmacol. Toxicol. 44 (2004) 239–267.
[3] O.A. Sedelnikova, C.E. Redon, J.S. Dickey, A.J. Nakamura, A.G. Georgakilas, W.M. Bonner, Role of oxidatively induced DNA lesions in human pathogenesis, Mutat. Res. 704 (2010) 152–159.
[4] H. Tsutsui, S. Kinugawa, S. Matsushima, Oxidative stress and heart failure, Am. J. Physiol. Heart Circ. Physiol. 301 (2011) H2181–H2190.
[5] M.L. Hegde, A.K. Mantha, T.K. Hazra, K.K. Bhakat, S. Mitra, B. Szczesny, Oxidative genome damage and its repair: implications in aging and neurodegenerative diseases, Mech. Ageing Dev. 133 (2012) 157–168.
[6] T.B. Kryston, A.B. Georgiev, P. Pissis, A.G. Georgakilas, Role of oxidative stress and DNA damage in human carcinogenesis, Mutat. Res. 711 (2011) 193–201.
[7] S.S. David, V.L. O'Shea, S. Kundu, Base-excision repair of oxidative DNA damage, Nature 447 (2007) 941–950.
[8] D. Svilar, E.M. Goellner, K.H. Almeida, R.W. Sobol, Base excision repair and lesion-dependent subpathways for repair of oxidative DNA damage, Antioxid. Redox Signal. 14 (2011) 2491–2507.
[9] W. Luo, J.G. Muller, E.M. Rachlin, C.J. Burrows, Characterization of spiroiminodihydantoin as a product of one-electron oxidation of 8-oxo-7,8-dihydroguanosine, Org. Lett. 2 (2000) 613–616.
[10] W. Luo, J.G. Muller, E.M. Rachlin, C.J. Burrows, Characterization of hydantoin products from one-electron oxidation of 8-oxo-7,8-dihydroguanosine in a nucleoside model, Chem. Res. Toxicol. 14 (2001) 927–938.
[11] T. Suzuki, T. Inoue, M. Inukai, Formation of spiroiminodihydantoin nucleosides from 8-oxo-7,8-dihydro-2′-deoxyguanosine by ultraviolet light, Genes Environ. 32 (2010) 31–36.
[12] T. Suzuki, Formation of spiroiminodihydantoin nucleoside from 8-oxo-7,8-dihydro-2′-deoxyguanosine by nitric oxide under aerobic conditions, Bioorg. Med. Chem. Lett. 19 (2009) 4944–4947.
[13] K. Kino, M. Morikawa, T. Kobayashi, T. Kobayashi, R. Komori, Y. Sei, H. Miyazawa, The oxidation of 8-oxo-7,8-dihydroguanine by iodine, Bioorg. Med. Chem. Lett. 20 (2010) 3818–3820.
[14] P.T. Henderson, J.C. Delaney, J.G. Muller, W.L. Neeley, S.R. Tannenbaum, C.J. Burrows, J.M. Essigmann, The hydantoin lesions formed from oxidation of 7,8-dihydro-8-oxoguanine are potent sources of replication errors in vivo, Biochemistry 42 (2003) 9257–9262.
[15] H. Dou, S. Mitra, T.K. Hazra, Repair of oxidized bases in DNA bubble structures by human DNA glycosylases NEIL1 and NEIL2, J. Biol. Chem. 278 (2003) 49679–49684.
[16] M.K. Hailer, P.G. Slade, B.D. Martin, T.A. Rosenquist, K.D. Sugden, Recognition of the oxidized lesions spiroiminodihydantoin and guanidinohydantoin in DNA by the mammalian base excision repair glycosylases NEIL1 and NEIL2, DNA Repair 4 (2005) 41–50.
[17] N. Krishnamurthy, X. Zhao, C.J. Burrows, S.S. David, Superior removal of hydantoin lesions relative to other oxidized bases by the human DNA glycosylase hNEIL1, Biochemistry 47 (2008) 7137–7146.
[18] M. Liu, V. Bandaru, J.P. Bond, P. Jaruga, X. Zhao, P.P. Christov, C.J. Burrow, C.J. Rizzo, M. Dizdaroglu, S.S. Wallace, The mouse ortholog of NEIL3 is a functional DNA glycosylase in vitro and in vivo, Proc. Natl. Acad. Sci. U. S. A. 107 (2010) 4925–4930.
[19] X. Zhao, N. Krishnamurthy, C.J. Burrows, S.S. David, Mutation versus repair: NEIL1 removal of hydantoin lesions in single-stranded, bulge, bubble, and duplex DNA contexts, Biochemistry 49 (2010) 1658–1666.
[20] M. Redrejo-Rodríguez, C. Saint-Pierre, S. Couve, A. Mazouzi, A.A. Ishchenko, D. Gasparutto, M. Saparbaev, New insights in the removal of the hydantoins, oxidation product of pyrimidines, via the base excision and nucleotide incision repair pathways, PLoS One 6 (2011) e21039.
[21] J.P. Radicella, C. Dherin, C. Desmaze, M.S. Fox, S. Boiteux, Cloning and characterization of hOGG1, a human homolog of the OGG1 gene of Saccharomyces cerevisiae, Proc. Natl. Acad. Sci. U. S. A. 94 (1997) 8010–8015.
[22] K. Imai, A.H. Sarker, K. Akiyama, S. Ikeda, M. Yao, K. Tsutsui, T. Shohmori, S. Seki, Genomic structure and sequence of a human homologue (NTHL1/NTH1) of Escherichia coli endonuclease III with those of the adjacent parts of TSC2 and SLC9A3R2 genes, Gene 222 (1998) 287–295.
[23] A.H. Sarker, S. Ikeda, H. Nakano, H. Terato, H. Ide, K. Imai, K. Akiyama, K. Tsutsui, Z. Bo, K. Kubo, K. Yamamoto, A. Yasui, M.C. Yoshida, S. Seki, Cloning and characterization of a mouse homologue (mNthl1) of Escherichia coli endonuclease III, J. Mol. Biol. 282 (1998) 761–774.
[24] I. Morland, V. Rolseth, L. Luna, T. Rognes, M. Bjørås, E. Seeberg, Human DNA glycosylases of the bacterial Fpg/MutM superfamily: an alternative pathway for the repair of 8-oxoguanine and other oxidation products in DNA, Nucleic Acids Res. 30 (2002) 4926–4936.
[25] T.K. Hazra, T. Izumi, I. Boldogh, B. Imhoff, Y.W. Kow, P. Jaruga, M. Dizdaroglu, S. Mitra, Identification and characterization of a human DNA glycosylase for repair of modified bases in oxidatively damaged DNA, Proc. Natl. Acad. Sci. U. S. A. 99 (2002) 3523–3528.
[26] T.K. Hazra, Y.W. Kow, Z. Hatahet, B. Imhoff, I. Boldogh, S.K. Mokkapati, S. Mitra, T. Izumi, Identification and characterization of a novel human DNA glycosylase for repair of cytosine-derived lesions, J. Biol. Chem. 277 (2002) 30417–30420.
[27] K. Torisu, D. Tsuchimoto, Y. Ohnishi, Y. Nakabeppu, Hematopoietic tissue-specific expression of mouse Neil3 for endonuclease VIII-like protein, J. Biochem. 138 (2005) 763–772.
[28] G.A. Hildrestrand, D.B. Diep, D. Kunke, N. Bolstad, M. Bjørås, S. Krauss, L. Luna, The capacity to remove 8-oxoG is enhanced in newborn neural stem/progenitor cells and decreases in juvenile mice and upon cell differentiation, DNA Repair 6 (2007) 23–732.
[29] V. Rolseth, E. Rundén-Pran, L. Luna, C. McMurray, M. Bjørås, O.P. Ottersen, Widespread distribution of DNA glycosylases removing oxidative DNA lesions in human and rodent brains, DNA Repair 7 (2008) 1578–1588.
[30] G.A. Hildrestrand, C.G. Neurauter, D.B. Diep, C.G. Castellanos, S. Krauss, M. Bjørås, L. Luna, Expression patterns of Neil3 during embryonic brain development and neoplasia, BMC Neurosci. 10 (2009) 45, (9).
[31] M. Takao, Y. Oohata, K. Kitadokoro, K. Kobayashi, S. Iwai, A. Yasui, S. Yonei, Q.M. Zhang, Human Nei-like protein NEIL3 has AP lyase activity specific for single-stranded DNA and confers oxidative stress resistance in Escherichia coli mutant, Genes Cells 14 (2009) 261–270.
[32] C.G. Neurauter, L. Luna, M. Bjørås, Release from quiescence stimulates the expression of human NEIL3 under the control of the Ras dependent ERK-MAP kinase pathway, DNA Repair 11 (2012) 401–409.
[33] A. Klungland, I. Rosewell, S. Hollenbach, E. Larsen, G. Daly, B. Epe, E. Seeberg, T. Lindahl, D.E. Barnes, Accumulation of premutagenic DNA lesions in mice defective in removal of oxidative base damage, Proc. Natl. Acad. Sci. U. S. A. 96 (1999) 13300–13305.

[34] O. Minowa, T. Arai, M. Hirano, Y. Monden, S. Nakai, M. Fukuda, M. Itoh, H. Takano, Y. Hippou, H. Aburatani, K. Masumura, T. Nohmi, S. Nishimura, T. Noda, Mmh/Ogg1 gene inactivation results in accumulation of 8-hydroxyguanine in mice, Proc. Natl. Acad. Sci. U. S. A. 97 (2000) 4156–4161.

[35] M.T. Ocampo, W. Chaung, D.R. Marenstein, M.K. Chan, A. Altamirano, A.K. Basu, R.J. Boorstein, R.P. Cunningham, G.W. Teebor, Targeted deletion of mNth1 reveals a novel DNA repair enzyme activity, Mol. Cell. Biol. 22 (2002) 6111–6121.

[36] M. Takao, S. Kanno, T. Shiromoto, R. Hasegawa, H. Ide, S. Ikeda, A.H. Sarker, S. Seki, J.Z. Xing, X.C. Le, M. Weinfeld, K. Kobayashi, J. Miyazaki, M. Muijtjens, J.H. Hoeijmakers, G. van der Horst, A. Yasui, Novel nuclear and mitochondrial glycosylases revealed by disruption of the mouse Nth1 gene encoding an endonuclease III homolog for repair of thymine glycols, EMBO J. 21 (2002) 3486–3493.

[37] B. Karahalil, N.C. de Souza-Pinto, J.L. Parsons, R.H. Elder, V.A. Bohr, Compromised incision of oxidized pyrimidines in liver mitochondria of mice deficient in NTH1 and OGG1 glycosylases, J. Biol. Chem. 278 (2003) 33701–33707.

[38] V. Vartanian, B. Lowell, I.G. Minko, T.G. Wood, J.D. Ceci, S. George, S.W. Ballinger, C.L. Corless, A.K. McCullough, R.S. Lloyd, The metabolic syndrome resulting from a knockout of the NEIL1 DNA glycosylase, Proc. Natl. Acad. Sci. U. S. A. 103 (2006) 1864–1869.

[39] Y. Sejersted, G.A. Hildrestrand, D. Kunke, V. Rolseth, S.Z. Krokeide, C.G. Neurauter, R. Suganthan, M. Atneosen-Åsegg, A.M. Fleming, O.D. Saugstad, C.J. Burrows, L. Luna, M. Bjørås, Endonuclease VIII-like 3 (Neil3) DNA glycosylase promotes neurogenesis induced by hypoxia–ischemia, Proc. Natl. Acad. Sci. U. S. A. 108 (2011) 18802–18807.

[40] D. Liu, D.L. Croteau, N. Souza-Pinto, M. Pitta, J. Tian, C. Wu, H. Jiang, K. Mustafa, G. Keijzers, V.A. Bohr, M.P. Mattson, Evidence that OGG1 glycosylase protects neurons against oxidative DNA damage and cell death under ischemic conditions, J. Cereb. Blood Flow Metab. 31 (2011) 680–692.

[41] C. Canugovi, J.S. Yoon, N.H. Feldman, D.L. Croteau, M.P. Mattson, V.A. Bohr, Endonuclease VIII-like 1 (NEIL1) promotes short-term spatial memory retention and protects from ischemic stroke-induced brain dysfunction and death in mice, Proc. Natl. Acad. Sci. U. S. A. 109 (2012) 14948–14953.

[42] O. Machon, C.J. van den Bout, M. Backman, O. Rosok, X. Caubit, S.H. Fromm, B. Geronimo, S. Krauss, Forebrain-specific promoter/enhancer D6 derived from the mouse Dach1 gene controls expression in neural stem cells, Neuroscience 112 (2002) 951–966.

[43] G. Rappa, D. Kunke, J. Holter, D.B. Diep, J. Meyer, C. Baum, O. Fodstad, S. Krauss, A. Lorico, Efficient expansion and gene transduction of mouse neural stem/progenitor cells on recombinant fibronectin, Neuroscience 124 (2004) 823–830.

[44] M. Takao, S. Kanno, K. Kobayashi, Q.M. Zhang, S. Yonei, G.T. van der Horst, A. Yasui, A back-up glycosylase in Nth1 knock-out mice is a functional Nei (endonuclease VIII) homologue, J. Biol. Chem. 277 (2002) 42205–42213.

[45] M.L. Dodson, M.L. Michaels, R.S. Lloyd, Unified catalytic mechanism for DNA glycosylases, J. Biol. Chem. 269 (1994) 32709–32712.

[46] M.L. Dodson, R.D. Schrock, S. Lloyd, Evidence for an imino intermediate in the T4 endonuclease V reaction, Biochemistry 32 (1993) 8284–8290.

[47] S.Z. Krokeide, N. Bolstad, J.K. Laerdahl, M. Bjørås, L. Luna, Expression and purification of NEIL3, a human DNA glycosylase homolog, Protein Expr. Purif. 65 (2009) 160–164.

[48] A.D. Tramontin, J.M. García-Verdugo, D.A. Lim, A. Alvarez-Buylla, Postnatal development of radial glia and the ventricular zone (VZ): a continuum of the neural stem cell compartment, Cereb. Cortex 13 (2003) 580–587.

[49] A. Kriegstein, A. Alvarez-Buylla, The glial nature of embryonic and adult neural stem cells, Annu. Rev. Neurosci. 32 (2009) 149–184.

[50] H. Georg Kuhn, K. Blomgren, Developmental dysregulation of adult neurogenesis, Eur. J. Neurosci. 33 (2011) 1115–1122.

[51] P. Taupin, BrdU immunohistochemistry for studying adult neurogenesis: paradigms, pitfalls, limitations, and validation, Brain Res. Rev. 53 (2007) 198–214.

[52] F. Lopez, F. Belloc, F. Lacombe, P. Dumain, J. Reiffers, P. Bernard, M.R. Boisseau, Modalities of synthesis of Ki67 antigen during the stimulation of lymphocytes, Cytometry 12 (1991) 42–49.

[53] A. Zacchetti, E. van Garderen, E. Teske, H. Nederbragt, J.H. Dierendonck, G.R. Rutteman, Validation of the use of proliferation markers in canine neoplastic

and non-neoplastic tissues: comparison of KI-67 and proliferating cell nuclear antigen (PCNA) expression *versus in vivo* bromodeoxyuridine labelling by immunohistochemistry, APMIS 111 (2003) 430–438.

[54] P. Kurki, M. Vanderlaan, F. Dolbeare, J. Gray, E.M. Tan, Expression of proliferating cell nuclear antigen (PCNA)/cyclin during the cell cycle, Exp. Cell Res. 166 (1986) 209–219.

[55] M.J. Hendzel, Y. Wei, M.A. Mancini, A. Van Hooser, T. Ranalli, B.R. Brinkley, D.P. Bazett-Jones, C.D. Allis, Mitosis-specific phosphorylation of histone H3 initiates primarily within pericentromeric heterochromatin during G2 and spreads in an ordered fashion coincident with mitotic chromosome condensation, Chromosoma 106 (1997) 348–360.

[56] F. Francis, A. Koulakoff, D. Boucher, P. Chafey, B. Schaar, M.C. Vinet, G. Friocourt, N. McDonnell, O. Reiner, A. Kahn, S.K. McConnell, Y. Berwald-Netter, P. Denoulet, J. Chelly, Doublecortin is a developmentally regulated, microtubule-associated protein expressed in migrating and differentiating neurons, Neuron 23 (1999) 247–256.

[57] J.G. Gleeson, P.T. Lin, L.A. Flanagan, C.A. Walsh, Doublecortin is a microtubule-associated protein and is expressed widely by migrating neurons, Neuron 23 (1999) 257–271.

[58] M. Liu, V. Bandaru, A. Holmes, A.M. Averill, W. Cannan, S.S. Wallace, Expression and purification of active mouse and human NEIL3 proteins, Protein Expr. Purif. 84 (2012) 130–139.

[59] C.E. Regnell, G.A. Hildrestrand, Y. Sejersted, T. Medin, O. Moldestad, V. Rolseth, S.Z. Krokeide, R. Suganthan, L. Luna, L.H. Bergersen Hippocampal, Adult neurogenesis is maintained by Neil3-dependent repair of oxidative DNA lesions in neural progenitor cells, Cell Rep. 2 (2012) 503–510.

[60] A. Reis, O. Hermanson, The DNA glycosylases OGG1 and NEIL3 influence differentiation potential, proliferation, and senescence-associated signs in neural stem cells, Biochem. Biophys. Res. Commun. 423 (2012) 621–626.

[61] T.K. Chang, F.S. Abbott, Oxidative stress as a mechanism of valproic acid-associated hepatotoxicity, Drug Metab. Rev. 38 (2006) 627–639.

[62] J.M. Morán, M.A. Ortiz-Ortiz, L.M. Ruiz-Mesa, J.M. Fuentes, Nitric oxide in paraquat-mediated toxicity: a review, J. Biochem. Mol. Toxicol. 24 (2010) 402–409.

[63] V. Cepeda, M.A. Fuertes, J. Castilla, C. Alonso, C. Quevedo, J.M. Pérez, Biochemical mechanisms of cisplatin cytotoxicity, Anticancer Agents Med Chem. 7 (2007) 3–18.

[64] D.G. Deavall, E.A. Martin, J.M. Horner, R. Roberts, Drug-induced oxidative stress and toxicity, J. Toxicol. 2012 (2012) 655460.

[65] M.A. Lemaire, A. Schwartz, A.R. Rahmouni, M. Leng, Interstrand cross-links are preferentially formed at the d(GC) sites in the reaction between cis-diamminedichloroplatinum (II) and DNA, Proc. Natl. Acad. Sci. U. S. A. 88 (1991) 1982–1985.

[66] P.B. Hopkins, J.T. Millard, J. Woo, M.F. Weidner, J.J. Kirchner, S.T. Sigmasson, S. Raucher, Sequence preferences of DNA interstrand cross-linking agents: importance of minimal DNA structural reorganization in the cross-linking reactions of mechlorethamine, cisplatin and mitomycin, Tetrahedron 47 (1991) 2475–2489.

[67] E.M. Hlavin, M.B. Smeaton, P.S. Miller, Initiation of DNA interstrand cross-link repair in mammalian cells, Environ. Mol. Mutagen. 51 (2010) 604–624.

[68] M. Enoiu, J. Jiricny, O.D. Schärer, Repair of cisplatin-induced DNA interstrand crosslinks by a replication-independent pathway involving transcription-coupled repair and translesion synthesis, Nucleic Acids Res. 40 (2012) 8953–8964.

[69] S. Couvé-Privat, G. Macé, F. Rosselli, M.K. Saparbaev, Psoralen-induced DNA adducts are substrates for the base excision repair pathway in human cells, Nucleic Acids Res. 35 (2007) 5672–5682.

[70] S. Couvé, G. Macé-Aimé, F. Rosselli, M.K. Saparbaev, The human oxidative DNA glycosylase NEIL1 excises psoralen-induced interstrand DNA cross-links in a three-stranded DNA structure, J. Biol. Chem. 284 (2009) 11963–11970.

[71] G. Macé-Aimé, S. Couvé, B. Khassenov, F. Rosselli, M.K. Saparbaev, The Fanconi anemia pathway promotes DNA glycosylase-dependent excision of interstrand DNA crosslinks, Environ. Mol. Mutagen. 51 (2010) 508–519.

[72] S. L'Espérance, M. Bachvarova, B. Tetu, A.M. Mes-Masson, D. Bachvarov, Global gene expression analysis of early response to chemotherapy treatment in ovarian cancer spheroids, BMC Genomics 9 (2008) 99.